Biochimica et Biophysica Acta 1801 (2010) 1294–1304

Contents lists available at ScienceDirect

Biochimica et Biophysica Acta

journal homepage: www.elsevier.com/locate/bbalip

Visfatin-induced lipid raft redox signaling platforms and dysfunction in glomerular endothelial cells

Krishna M. Boini, Chun Zhang, Min Xia, Wei-Qing Han, Christopher Brimson, Justin L. Poklis, Pin-Lan Li *

Department of Pharmacology and Toxicology, Medical College of Virginia Campus, Virginia Commonwealth University, Richmond, VA, 23298, USA

ARTICLE INFO

Article history:
Received 24 January 2010
Received in revised form 16 August 2010
Accepted 14 September 2010
Available online 19 September 2010

Keywords:
Lipid membrane microdomain
Glomerulus
Redox regulation
Free radical
Adipokine
Sphingolipid

ABSTRACT

Adipokines have been reported to contribute to glomerular injury during obesity or diabetes mellitus. However, the mechanisms mediating the actions of various adipokines on the kidney remained elusive. The present study was performed to determine whether acid sphingomyelinase (ASM)-ceramide associated lipid raft (LR) clustering is involved in local oxidative stress in glomerular endothelial cells (GECs) induced by adipokines such as visfatin and adiponectin. Using confocal microscopy, visfatin but not adiponectin was found to increase LRs clustering in the membrane of GECs in a dose and time dependent manner. Upon visfatin stimulation ASMase activity was increased, and an aggregation of ASMase product, ceramide and NADPH oxidase subunits, $gp91^{phox}$ and $p47^{phox}$ was observed in the LR clusters, forming a LR redox signaling platform. The formation of this signaling platform was blocked by prior treatment with LR disruptor filipin, ASMase inhibitor amitriptyline, ASMase siRNA, $gp91^{phox}$ siRNA and adiponectin. Corresponding to LR clustering and aggregation of NADPH subunits, superoxide ($O_2^{\bullet -}$) production was significantly increased (2.7 folds) upon visfatin stimulation, as measured by electron spin resonance (ESR) spectrometry. Functionally, visfatin significantly increased the permeability of GEC layer in culture and disrupted microtubular networks, which were blocked by inhibition of LR redox signaling platform formation. In conclusion, the injurious effect of visfatin, but not adiponectin on the glomerular endothelium is associated with the formation of LR redox signaling platforms via LR clustering, which produces local oxidative stress resulting in the disruption of microtubular networks in GECs and increases the glomerular permeability.

1. Introduction

The increasing incidence of obesity leading to metabolic complications or metabolic syndrome is now recognized as a major public health problem. Adipose tissue as an active metabolic tissue secretes multiple metabolically important proteins known as 'adipokines'. Some adipokines play a major role in insulin resistance and cardiovascular complications associated with obesity, especially central or visceral obesity [1,2]. In this regard, adiponectin is a protein highly expressed in adipose tissue, which has been shown to improve insulin sensitivity in the liver [3] and periphery [4], ameliorate endothelial dysfunction [5], and counteract pro-inflammatory signaling [5]. These actions of adiponectin are proposed to be involved in an autoregulatory mechanism whereby the detrimental effects of obesity would be ameliorated [6]. A low circulating level of adiponectin is generally found in populations at enhanced risk of cardiovascular diseases [7,8], and reduced adiponectin levels predispose healthy individuals to the later development of insulin resistance [8]. In patients with chronic kidney diseases (CKD), plasma adiponectin levels have been reported to be markedly elevated [9,10], and CKD patients with low plasma adiponectin levels have an increased risk of cardiovascular events [10], suggesting a protective role of adiponectin in the development of CKD.

Another novel adipokine visfatin has also been mainly expressed in visceral adipose tissue [11]. Previously visfatin was identified as Pre-B colony Enhancing Factor (PBEF), a growth factor involved in the early development of B lymphocytes [12]. Visfatin was reported as a highly expressed protein with insulin-like functions. However some later reports could not confirm these functions in humans [13,14]. The validity of insulin-mimetic properties of visfatin is under debate at present [15]. The initial observations were partially retracted [16]. Furthermore, elevated plasma levels of visfatin were found in patients with type 2 [17] and type 1 diabetes mellitus that can be lowered by regular physical exercise [18]. A significant association between two visfatin gene variants and plasma insulin levels was reported [19]. Recent studies have confirmed that visfatin is, indeed, an adipokine which may be involved in the development of various obesity-associated pathologies [17,20–27]. Visfatin has been implicated as a nicotinamide phosphoribosyltransferase (Nampt), which regulates nicotinamide adenine dinucleotide (NAD^+)-dependent protein

* Corresponding author. Department of Pharmacology and Toxicology, Medical College of Virginia Campus, Virginia Commonwealth University, 1220 East Broad St, MMRB, Room # 3054, Richmond, VA, 23298, USA. Tel.: +1 804 828 4793; fax: +1 804 828 4794.
E-mail address: pli@vcu.edu (P.-L. Li).

1388-1981/$ – see front matter © 2010 Elsevier B.V. All rights reserved.
doi:10.1016/j.bbalip.2010.09.001

deacetylase activity when it works as a dimer [24]. It has been postulated that visfatin may play a role in innate immunity during inflammation and obesity (a low-grade inflammatory process). Visfatin expression and plasma levels of visfatin are associated with obesity in animals and humans [11,28]. Furthermore, the plasma levels of visfatin were significantly increased in high fat diet fed mice compared to normal chow fed mice. Visfatin treatment in diabetic mice improved insulin sensitivity, with the insulin-mimetic action of visfatin mediated through binding to the insulin receptor [11,16].

Recent studies have also reported that plasma visfatin level was significantly increased from 29 ng/mL in normal controls to 41 ng/mL in a large population of patients with CKD [29]. In contrast to adiponectin, the higher the plasma levels of visfatin, the more severe the CKD, and a higher plasma level of visfatin predicts a higher mortality rate in these patients of CKD. There may be a couple of reasons for the increase of visfatin levels in the patients with CKD. It may be due to the chronic inflammation associated with this disease or hypoxia as a result of tubulonecrosis, anaemia, decreased capillary flow or it may be because of increased diffusion lengths due to deposition of the extracellular matrix [30]. Although elevated plasma visfatin levels have been demonstrated to play a role in the pathogenesis of diabetic nephropathy [31,32], it remains unknown how this adipokine acts in damaging glomeruli resulting in glomerular injury and ultimate glomerular sclerosis or end-stage renal disease.

Recently, we have reported that lipid raft (LR) clustering importantly participate in the development of endothelial dysfunction in coronary arteries, which is associated with the formation of LR redox signaling platforms [33]. These signaling platforms in the membrane of coronary arterial endothelial cells are characterized by $gp91^{phox}$ and $p47^{phox}$ aggregation in LR clusters and enhanced NADPH oxidase activity, when these cells were stimulated by different death receptor ligands. It was shown that acid sphingomyelinase (ASM) and ceramide production resulted in the formation of such LR redox signaling platforms [33]. The present study hypothesized that adipokines such as visfatin and adiponectin may induce ceramide production via ASMase activation and thereby stimulates LR clustering in the membrane of GECs to form redox signaling platforms by aggregation and activation of NADPH oxidase subunits, enhancing $O_2^{\bullet -}$ production and leading to GEC dysfunction and ultimate glomerular injury.

To test this hypothesis, we first determined whether adipokines stimulate LR clustering to form redox signaling platforms with aggregation and activation of NADPH oxidase subunits in GEC membrane using confocal microscopy. We also determined the contribution of this LR redox signaling platform formation to endothelial dysfunction associated with visfatin by examining their actions on the permeability of GEC layer preparations. Furthermore, we determined whether visfatin-induced LR redox signaling platform formation is associated with the regulation of microtubular network stability in these cells, a critical factor for the maintenance of endothelial barrier function.

2. Materials and methods

2.1. Cell culture

The GEC colony used in the present study was a kind gift from Dr. Masaomi Nangaku, University of Tokyo, School of Medicine and Dr. Stephen Adler, New York Medical College. The cells were isolated and cloned as reported previously [34]. In brief, these cells were isolated from glomeruli of male Sprague–Dawley rats and then cultured and frozen for use at passage 3 or 4. The characteristics of these cells were kept such as positive staining with JG12, but negative labeling of podocalyxin, nephrin, α-smooth muscle actin, and ED-1. These cells were maintained in RPMI 1640 containing 2000 mg/L glucose, supplemented with 10% fetal bovine serum (FBS) (JRH Biosciences, Lenexa, KS, USA) and 10% NuSerum (BD Biosciences, Bedford, MA, USA) at 37 °C under a humidified atmosphere of 5% CO_2/95% air for use.

2.2. Confocal microscopy of LR clusters and its colocalization with ceramide and NADPH oxidase subunits in GECs

For confocal microscopic detection of LRs and their associated proteins, GECs were grown on poly-L-lysine-coated chambers and treated with visfatin (2 μg/mL, 6 h, BioVision, Mountain View, CA). In additional group of cells, the LR disruptor, filipin (1 μg/mL, Sigma, St. Louis, MO, USA), NADPH oxidase inhibitor, DPI (10 μm, Sigma, St. Louis, MO, USA), adiponectin (6 μg/mL, Phoenix Pharmaceuticals, Burlingame, CA), amitriptyline (20 μm, Sigma, St. Louis, MO, USA), ASMase siRNA (Qiazen, Valencia, CA) and $gp91^{phox}$ siRNA (Qiazen, Valencia, CA) were added to pretreat the cells for 30 min before addition of visfatin. Detection of LR clusters was performed as we described previously [33,35,36]. Briefly, cells were washed with cold PBS, fixed for 15 min with 4% paraformaldehyde (PFA) and then blocked with 1% BSA in PBS for 30 min. GM1 gangliosides enriched in LRs were stained with Alexa488-labeled cholera toxin (CTX; 1 μg/mL, Molecular Probes, Carlsbad, CA, USA) for 30 min. The patch formation of Alexa488-labeled CTX and gangliosides complex represented the clusters of LRs. Clustering was defined as 1 or several intense spots of fluorescence on the cell surface, whereas unstimulated cells displayed a homogenous distribution of fluorescence throughout the membrane. For detection of the colocalization of LRs and ceramide or NADPH oxidase subunits anti-$gp91^{phox}$, anti-$p47^{phox}$, and GECs were incubated overnight with indicated primary monoclonal mouse antibodies (1:100, BD bioscience), followed by incubation with 5 μg/mL Texas Red conjugated anti-mouse antibody for an additional 1 h at room temperature. After mounting, the slides were observed using a confocal laser scanning microscope (Fluoview FV1000, Olympus, Japan). In each experiment, the presence or absence of clustering in samples of 200 cells was scored by 2 independent observers, and the results were given as the percentage of cells showing a cluster after the indicated treatment as described [33,35,36].

2.3. Liquid chromatography–electrospray ionization tandem mass spectrometry (LC–ESI–MS–MS) for quantitation of ceramide

Separation, identification and quantitation of ceramide in GECs were performed by LC/MS. The HPLC was equipped with a binary pump, a vacuum degasser, a thermostated column compartment and an autosampler (Waters, Milford, MA, USA). The HPLC separations were performed at 70 °C on a RP C18 Nucleosil AB column (5 μm, 70 mm × 2 mm i.d.) from Macherey Nagel (Düren, Germany). The mobile phase was a gradient mixture formed as described [37]. The cell lipids were extracted according to previous studies [38]. To avoid any loss of lipids, the whole procedure was performed in siliconized glassware. MS detection was carried out using a Quattro II quadrupole mass spectrometer (Micromass, Altrincham, England) operating under MassLynx 3.5 and configured with a Z-spray electrospray ionization source. Source conditions were described as previously [37].

2.4. Assay of sphingomyelinase activity

The activity of acid sphingomyelinase was determined as described previously [38]. Briefly, *N*-methyl-[^{14}C]-sphingomyelin was incubated with cell homogenates, and the metabolites of sphingomyelin, [^{14}C]-choline phosphate was quantified. An aliquot of homogenates (20 μg) was mixed with 0.02 μCi of *N*-methyl ^{14}C-sphingomyelin in 100 μL acidic reaction buffer containing 100 mmol/L sodium acetate, and 0.1% Triton X-100, pH 5.0, and incubated at 37 °C for 15 min. The reaction was terminated by adding 1.5 mL chloroform:methanol (2:1) and 0.2 mL

double-distilled water. The samples were then vortexed and centrifuged at 1000 ×*g* for 5 min to separate into two phases. A portion of the upper aqueous phase containing ^{14}C-choline phosphate was transferred to scintillation vials and counted in a Beckman liquid scintillation counter. The choline phosphate formation rate (nmol min^{-1} mg protein^{-1}) was calculated to represent the enzyme activity.

2.5. Flotation of membrane LR fractions

GECs were stimulated by addition of visfatin to the serum-free medium and incubated for 6 h. To isolate LR fractions from the cell membrane, these cells were lysed in 1.5 mL MBS buffer containing (in micromoles per liter) morpholinoethane sulfonic acid, 25; NaCl, 150; EDTA, 1; PMSF, 1; Na3VO4, 1; and a mixture of protease inhibitors and 1% Triton X-100 (pH 6.5). Cell extracts were homogenized by 5 passages through a 25-gauge needle. Then, homogenates were adjusted with 60% OptiPrep Density Gradient medium (Sigma, St. Louis, MO, USA) to 40% and overlaid with an equal volume (4.5 mL) of discontinuous 30%–5% OptiPrep Density Gradient medium. Samples were centrifuged at 32,000 rpm for 24 h at 4 °C using a SW32.1 rotor. Fractions were collected from the top to bottom. Then, these fractions were precipitated by mixing with an equal volume of 30% trichloroacetic acid and incubated for 30 min on ice. Precipitated proteins were spun down by centrifugation at 13,000 rpm at 4 °C for 15 min. The protein pellet was carefully washed once with cold acetone, air dried, and resuspended in 1 mol/L Tris–HCl (pH 8.0), which was used for Western blot analysis [39]. In brief, after boiled for 5 min at 95 °C in a 5′ loading buffer, samples were subjected to SDS-PAGE, transferred onto a PVDF membrane and blocked. Then, the membrane was probed with primary antibodies of anti-flotillin-1, a non-caveolar LR marker (1:1000, BD Biosciences, San Jose, CA), anti-gp91^{phox} (1:500, BD Biosciences, San Jose, CA) overnight at 4 °C followed by incubation with horseradish peroxidase-labeled IgG (1:5000). The immunoreactive bands were detected by chemiluminescence methods and visualized on Kodak Omat X-ray films. Densitometric analysis of the images obtained from X-ray films was performed using the Image J software (NIH, Bethesda, MD, USA).

2.6. Electronic spin resonance (ESR) analysis of O_2•$^-$ production in GECs

ESR detection of O_2•$^-$ was performed as we described previously [33,35,36]. In brief, gently collected GECs were suspended in modified Kreb's/HEPEs buffer containing deferroximine (25 mol/L, metal chelator). Approximately 1×10^6 GECs were mixed with 1 mmol/L spin trap 1-hydroxy-3-methoxycarbonyl-2,2,-5,5-tetrame-thylpyrrolidine (CMH) in the presence or absence of 100 U/mL polyethylene glycol (PEG)-conjugated superoxide dismutase (SOD). The cell mixture loaded in glass capillaries was immediately analyzed by ESR (Noxygen Science Transfer & Diagnostics GmbH, Denzlingen, Germany) for production of O_2•$^-$ at each minute for 10 min. The ESR settings were as follows: biofield, 3350; field sweep, 60 G; microwave frequency, 9.78 GHz; microwave power, 20 mW; modulation amplitude, 3 G; 4096 points of resolution; receiver gain, 500; and kinetic time, 10 min. The SOD-inhibitable signals were normalized by protein concentration and compared among different experimental groups. The relative increase in the ESR spectrum was used to represent NADPH oxidase activity.

2.7. Cell permeability assay

The permeability of GEC layer in culture was measured according to the methods as described previously [40,41]. In brief, GECs were seeded in the upper chambers of 0.4 μm polycarbonate Transwell filters of a 24-well filtration microplate (Whatman Inc.). After reaching confluence, the culture medium was replaced with fresh phenol red-free RPMI 1640 in the presence of visfatin and 70 kDa FITC-dextran (2.5 μmol/L) in the upper chambers. After visfatin treatment for 6 h, the filtration microplate was removed and the medium from the lower compartment was collected, and then fluorescence measured in a spectrofluorimeter at 494 nm excitation and 521 nm emission. The relative permeable fluorescence intensity was used to represent the cell permeability.

2.8. Immunofluorescent microscopic analysis of GEC cytoskeleton network

For detection of microtubule network analysis, GECs were treated with visfatin, alone or plus LR disruptor filipin, ASMase inhibitor amitriptyline, washed with phosphate-buffered saline (PBS; pH = 7.2), and then fixed. These cells were stained with anti-β-tubulin antibody (1:100; Abcam, Cambridge, MA, USA) after blocking with 1% bovine serum albumin (BSA; Sigma) in PBS for 30 min at RT, which was followed by washing cells four times with PBS. Finally, FITC-labeled secondary antibody was added, and cells were embedded into gelatine solution. Microtubule staining was analyzed using a Nikon ECLIPSE E 800 fluorescence microscope attached to a digital imaging system (Nikon, Tokyo, Japan).

For detection of visfatin-induced cytoskeleton changes, GECs were cultured in 8-well chambers and treated with or without stimulation of visfatin and washed with phosphate-buffered saline (PBS; pH = 7.2), and the cells were fixed in 4% paraformaldehyde for 15 min at room temperature, permeabilized with 0.1% Triton X-100, and blocked with 3% bovine serum albumin. F-actin was stained with rhodamine-phalloidin (Invitrogen, Carlsbad, CA, USA) for 15 min at room temperature. After mounting, the slides were examined using a Nikon ECLIPSE E 800 fluorescence microscope attached to a digital imaging system (Nikon, Tokyo, Japan).

2.9. Statistics

Data are provided as arithmetic means ± SEM, and n represents the number of independent cell batches for proposed experiments. All data were tested for significance using ANOVA, paired or unpaired Student t-test, as applicable. Only results with $p<0.05$ were considered statistically significant.

3. Results

3.1. Confocal microscopy of adipokine-induced LR clustering in GECs

As illustrated in Fig. 1A, typical fluorescent confocal microscopic images depict Alexa488-CTX-labeled patches on the cell membrane of GECs. Under the resting condition (control), there was only a diffuse fluorescent staining on the cell membrane, indicating a possible distribution of a single LR. When GECs were incubated with visfatin or FasL, a well-known stimulator of LR clustering in endothelial cells, some large fluorescent dots or patches were detected on the cell membrane, indicating LR patches or macrodomains. However, adiponectin had no effect on LR clustering. Fig. 1B summarized the effects of different doses of visfatin on the LR clustering by counting these LR clusters or patches. Under the control condition, GECs displayed a small percentage with LR clustering (3.9 ± 0.7%). After these cells were stimulated with visfatin, LR-clustered positive cells increased significantly in a dose dependent manner. At 2 μg/mL, visfatin increased LR clustering by 62.1 ± 10.2% ($P<0.05$, $n=5$). Adiponectin had no effect on such LR clustering in GECs (Fig. 1C). As positive control, FasL also induced significant clustering of LRs in GECs, confirming previous observations [33,42]. Additional experiments were performed to explore the time course of visfatin-induced LR clustering in GECs. It was found that visfatin treatment significantly increased the LR clustering in GECs after 3 h in a time dependent manner, reaching a striking increase of LR clustering at 6 h of visfatin treatment (Supplemental Fig. 1).

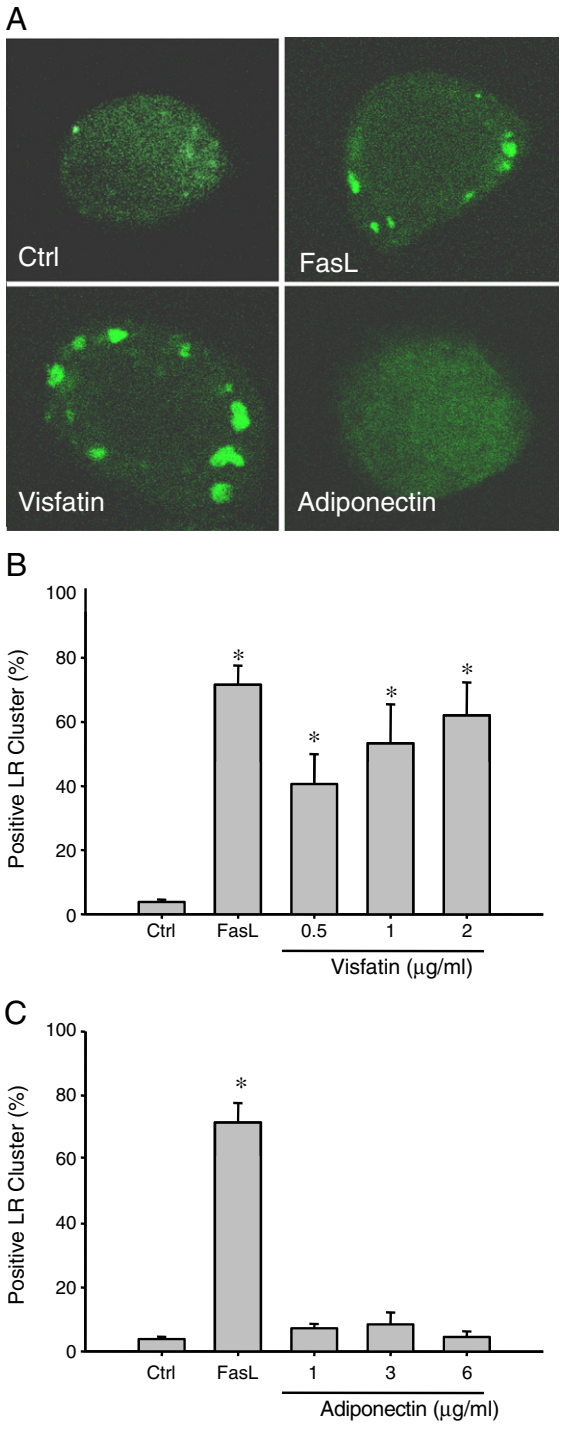

Fig. 1. Effects of adipokines on the LR clustering in the membrane of GECs. A) Representative confocal microscopic images of control, FasL, adiponectin and visfatin stimulated GECs stained with AL488-cholera toxin B (CTXB). B) Summarized data showing the effect of visfatin (0.5–2 μg/mL) and FasL on the formation of LR clusters. C) Summarized data showing the effect of adiponectin (1–6 μg/mL) and FasL on the formation of LR clusters. Panel bars displays means ± SEM of five experiments with analysis of more than 1000 GECs. *P<0.05 vs. control.

3.2. Quantitation of ceramide levels in visfatin-treated GECs

Previous studies in our laboratory have demonstrated that LR clustering triggered by ceramide occurs in coronary endothelial cells to form the redox signaling platforms, which mediates NADPH oxidase activation, resulting in increased $O_2^{\bullet -}$ production and endothelial dysfunction. Therefore, we examined whether visfatin also induces LR clustering due to its action on ceramide production. Using liquid chromatography/mass spectrometry analysis, we identified and quantified seven different major ceramides (C14, C16, C17, C18, C20, C22 and C24) in GECs with or without visfatin stimulation. Among them, C24 ceramide is the most abundant species. Visfatin treatment significantly increased the total ceramide levels after 4 h in a time dependent manner in the GECs upon visfatin stimulation compared to the untreated GECs (Supplemental Fig. 2).

3.3. Contribution of ceramide and ASMase to visfatin-induced LR clustering

To further confirm whether ceramide signaling is involved in visfatin-induced LR clustering and formation of redox signaling platforms, GECs were treated with visfatin and then first stained with Alexa488-labeled cholera toxin B (CTXB, a LR marker) followed by staining with anti-ceramide antibody and its second antibody conjugated with TRITC. As shown in Fig. 2A, LRs were evenly spread throughout the cell membrane under control condition as indicated by weak diffuse green FITC fluorescence in control cells, and there were no colocalization of LR and ceramide. Upon stimulation with visfatin, LRs were found to form clusters or multiple platforms as displayed by large and intense green fluorescence patches, which were stained by anti-ceramide antibody. However, adiponectin had no effect on such ceramide aggregation in LR clusters. Pretreatment of GECs with LR disruptor filipin, adiponectin, ASMase inhibitor amitriptyline or ASMase siRNA led to the disruption of LRs and abrogated patching and clustering of both FITC-CTXB and ceramide after visfatin stimulation. As depicted in Fig. 2B, the effects of visfatin, adiponectin, filipin, amitriptyline and Fasl on the LR clustering in cell membrane were summarized. In normal GECs there were only 10% of cells displayed with intense LR clusters, while 60% of cells showed clustering of LRs after stimulation with visfatin. Treatment of GECs with FasL, a positive control to stimulate LR clustering ECs, showed 76% positive cells. However, pretreatment of GECs with filipin, amitriptyline, adiponectin and ASMase siRNA showed that the visfatin-induced LR clustering was significantly blocked.

To further explore whether ASMase is involved in visfatin-induced LR clustering, we directly measured ASMase activity in GECs. As illustrated in Fig. 3, visfatin treatment for 6 h in GECs significantly increased the ASMase activity compared to untreated cells. However, pretreatment with LR disruptor filipin, adiponectin, ASMase inhibitor amitriptyline significantly attenuated the visfatin-induced increase in ASMase activity. Further experiments also confirmed that gene silencing of ASMase by siRNA significantly blocked the visfatin-induced ASMase activity. However, scrambled small RNA had no effects on the visfatin-induced ASMase activation in GECs (Fig. 3). Additional experiments were performed to explore the time course analysis of visfatin-induced ASMase activity in GECs. It was found that visfatin treatment significantly increased the ASMase activity in GECs after 2 h in a time dependent manner, reaching a striking increase of ASMase at 6 h of visfatin treatment (Supplemental Fig. 3).

3.4. Colocalization of $gp91^{phox}$ and $p47^{phox}$ with LR clusters and activation of NADPH oxidase upon visfatin stimulation

Earlier reports from our laboratory have demonstrated that FasL may induce the clustering of LRs on endothelial cell membrane and form redox signaling platforms, which contributes to the death receptor-induced endothelial dysfunction [42]. Therefore, we explored whether adipokines such as visfatin and adiponectin also induced LR clustering and subsequent aggregation and recruitment of NADPH oxidase subunits. In these experiments, GECs were treated with visfatin and stained with Alexa Fluo 488-labeled cholera toxin B (CTXB, a LR marker) and anti-$gp91^{phox}$ antibody to colocalize LRs and $gp91^{phox}$. As illustrated in Fig. 4A, both LRs and $gp91^{phox}$ were evenly distributed on the membrane of control cells. Upon visfatin stimulation, these LRs formed

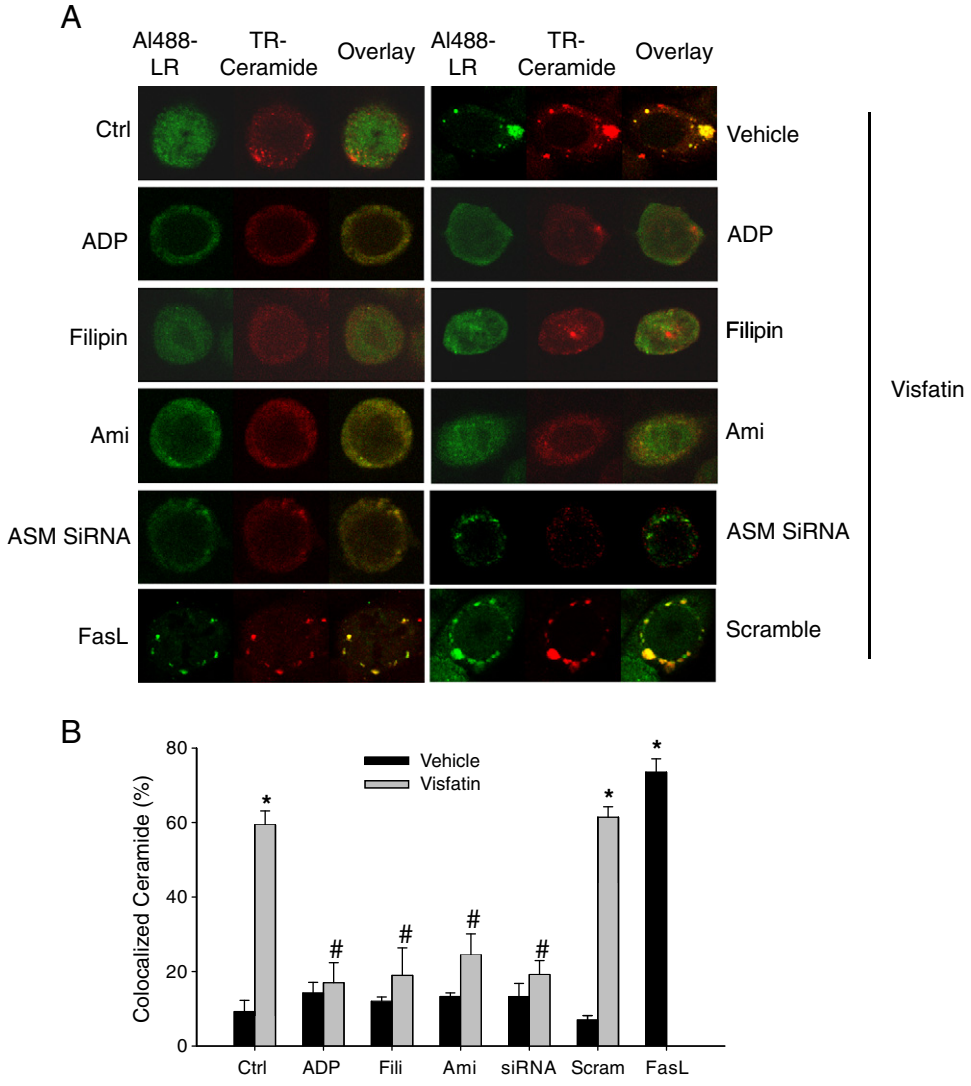

Fig. 2. Effects of adipokines on aggregation of ceramide and LR clusters in GECs. A) Representative confocal microscopic images of LR clusters and aggregation of ceramide in GECs. Alexa488-CTXB was shown as a green color on the left, Texas Red conjugated anti-ceramide antibody was shown as red color in the middle, and overlaid images were shown on the right. Yellow spots or patches in overlaid images were defined as LR clusters. B) Summarized data showing the effects of LR disruptor filipin, ASMase inhibitor amitriptyline and ASMase siRNA on the formation of LR-ceramide clusters. Panel bars display means ± SEM of five experiments with analysis of more than 1000 GECs. Ctrl: control, Ami: amitriptyline, Fili: filipin, siRNA: ASMase siRNA, Scram: scramble, and ADP: adiponectin. *P<0.05 vs. control; #P<0.05 vs. visfatin.

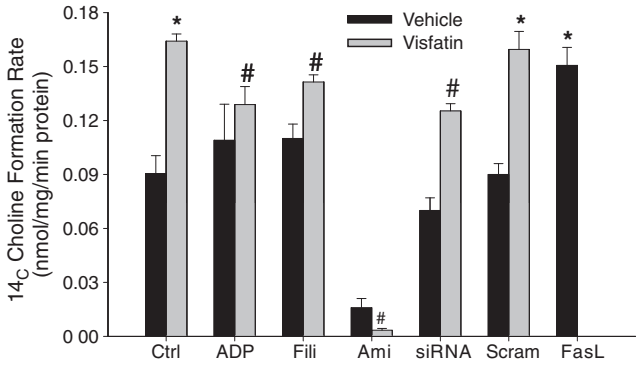

Fig. 3. Effects of adipokines on ASMase activity in GECs. Summarized data showing the conversion rate of ^{14}C-SM to ^{14}C-choline for measurement of ASMase activity. Values are means ± SEM from 5 to 6 separate experiments. Ctrl: control, Ami: amitriptyline, Fili: filipin, siRNA: ASMase siRNA, Scram: scramble, and ADP: adiponectin. *P<0.05 vs. control; #P<0.05 vs. visfatin.

large and intense green fluorescent patches, which were colocalized with gp91^{phox}. To examine whether these LR clusters are necessary for gp91^{phox} recruitment, we observed the effects of LR disruptor, filipin on visfatin-induced aggregation of gp91^{phox} in LR clusters. It was found that filipin significantly inhibited aggregation of gp91^{phox} in LR clusters. Furthermore, we addressed the effects of ASMase gene silencing or its inhibitor, amitriptyline on these aggregations of gp91^{phox} in LR clusters. We found that both the gene silencing of ASMase and ASMase inhibitor significantly attenuated the colocalization of gp91^{phox} and LRs. Additionally we tested the effects of NADPH oxidase inhibitor, DPI or gp91^{phox} siRNA on these aggregations of gp91^{phox} in LR clusters. We found that NADPH oxidase inhibitor, DPI or gene silencing of gp91^{phox} significantly attenuated the colocalization of gp91^{phox}, showing a feed forwarding regulation of LR clustering [33,43]. Unlike visfatin, adiponectin has no effect on the aggregation of gp91^{phox} in LR clusters. The effects of visfatin, adiponectin, filipin, DPI, amitriptyline and Fasl on the LR clustering in cell membrane were summarized as shown in Fig. 4B.

To further confirm the formation of LR-NADPH oxidase redox signaling complex, LR fractions were isolated and Western blot

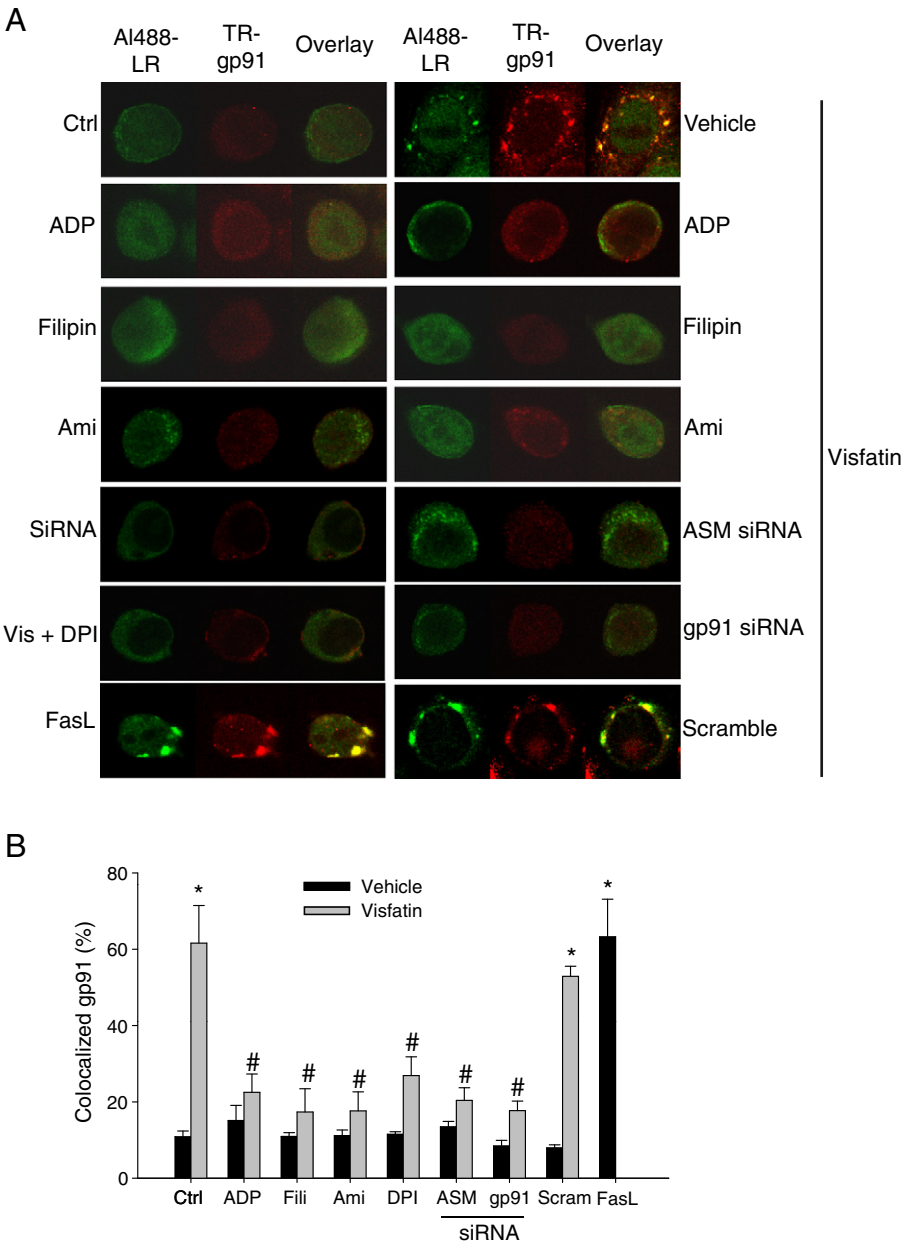

Fig. 4. Effects of adipokines on LR clustering and aggregation of gp91^{phox} in GECs. A) Representative confocal microscopic images of LR clusters and aggregation of gp91^{phox} in GECs. Alexa488-CTXB was shown as a green color on the left, Texas Red conjugated anti-gp91^{phox} antibody was shown as red color in the middle, and overlaid images were shown on the right. Yellow spots or patches in the overlaid images were defined as LR clusters with colocalization of gp91^{phox}. B) Summarized data showing the effects of LR disruptor, ASMase inhibitor, amitriptyline, ASMase siRNA, DPI and gp91^{phox} siRNA on the formation of LR-gp91^{phox} clusters. Panel bars display means ± SEM of five experiments with analysis of more than 1000 GECs. Ctrl: control, Ami: amitriptyline, Fili: filipin, Scram: scramble, and ADP: adiponectin. *P<0.05 vs. control; #P<0.05 vs. visfatin.

analysis was performed to detect gp91^{phox} protein. As shown in Fig. 5, a positive expression of flotillin-1 was present in fractions 4 to 6, which indicates a successful isolation of LR fractions. NADPH oxidase subunit, gp91^{phox} was detected in non-LR fractions in GECs under normal condition. However, stimulation of GECs with visfatin treatment significantly increased the gp91^{phox} protein in LR fractions compared to control GECs.

To examine whether LRs are also able to recruit cytosolic subunits such as p47^{phox} to form redox signaling platforms on the cell membrane, we stained GECs with Texas Red conjugated anti-p47^{phox} and Alexa Fluo 488-CTXB. As shown in Fig. 6, p47^{phox} was evenly distributed throughout the whole cell, mainly in cytosol under normal conditions. When these cells were treated with visfatin, translocated p47^{phox} on cell membrane were shown as red fluorescent spots or patches which were colocalized with CTXB, yielded a number of yellow areas either as dots or patches. These results indicate that p47^{phox} is translocated and associated with LR clusters. As expected, pretreatment with LR disruptor, filipin significantly attenuated the aggregation of p47^{phox} in LR clusters.

Additional experiments were performed to analyze NADPH oxidase activity by measurement of $O_2^{\bullet -}$ production in GECs and its influence by different inhibitors using ESR method. As illustrated in Fig. 7, visfatin significantly increased $O_2^{\bullet -}$ production in comparison to untreated cells. The increased production of $O_2^{\bullet -}$ induced by visfatin was significantly attenuated when GECs were pretreated with LR disruptor, filipin or gp91^{phox} siRNA, suggesting that LR associated NADPH oxidase subunits were the main source of $O_2^{\bullet -}$ production upon visfatin stimulation. Visfatin-induced $O_2^{\bullet -}$ production was also

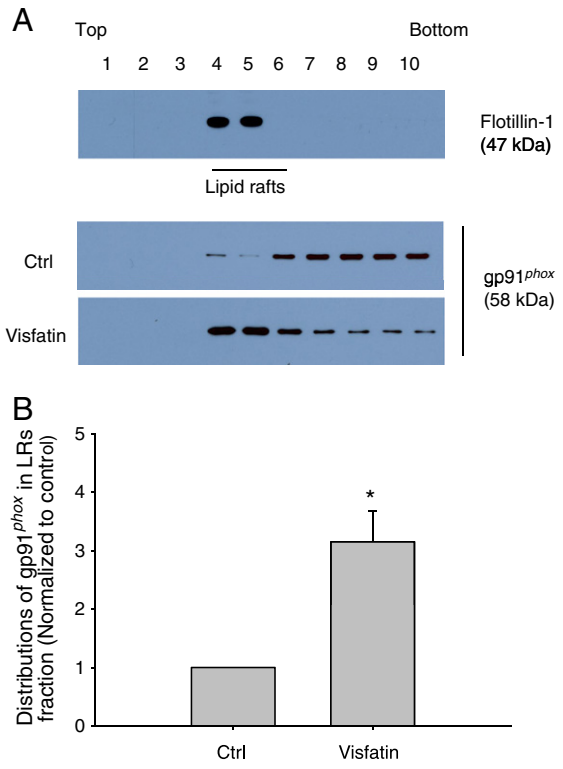

Fig. 5. Effect of visfatin on distribution and localization of $gp91^{phox}$ in floated membrane fractions from GECs. A) GECs were treated with or without stimulation of visfatin for 6 h. Numbers (1–10) on the top indicate membrane fractions isolated by gradient centrifugation from the top to bottom. Fractions 1–3 were very light fractions without proteins. Fractions 4–6 were light fractions designated as LR fractions as indicated by detection of the LR marker protein, flotillin-1. Other fractions from 7 to 10 were usually designated as non-raft fractions including membrane and cytosolic proteins. B) Densitometric analysis of the ratio of $gp91^{phox}$ in LR fractions to the total amount (LR/total). n = 3. *P<0.05 vs. control.

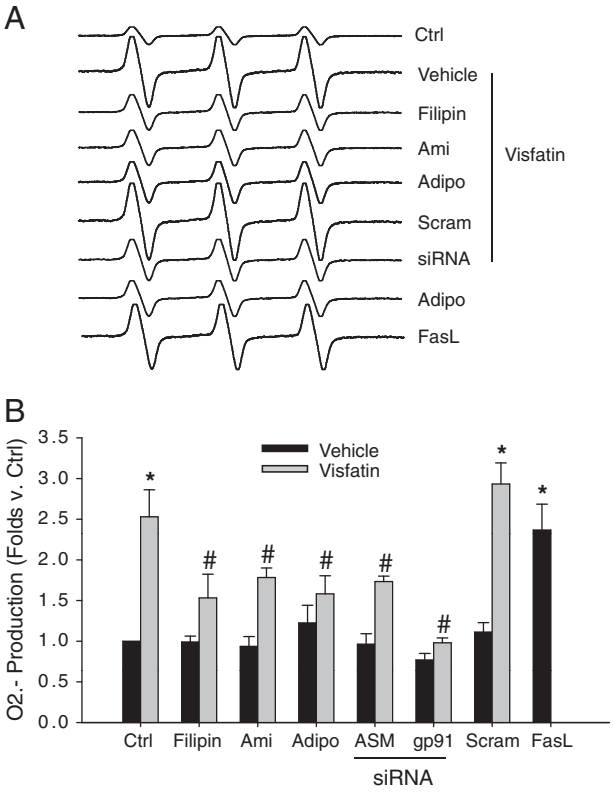

Fig. 7. Effects of adipokines on the $O_2^{\bullet -}$ production in GECs as measured by ESR spectrometry. A) Representative ESR spectra showing $O_2^{\bullet -}$ production in GECs under control condition and upon various stimulations. B) Summarized data showing the effects of adipokines on $O_2^{\bullet -}$ production. Values are means ± SEM, showing fold changes as compared with control. Ctrl: control, Ami: amitriptyline, Fili: filipin, Scram: scramble, and ADP: adiponectin. *P<0.05 vs. control; #P<0.05 vs. visfatin.

significantly attenuated by adiponectin, ASMase inhibitor amitriptyline or ASMase siRNA.

3.5. Blockade of visfatin-induced GEC monolayer permeability by disruption of LR clustering and ASMase gene silencing

To determine the role of LR clustering in mediating visfatin-induced GEC dysfunction, we examined its effect on the permeability of GEC monolayers to FITC-dextran. The possible effects of visfatin on the GEC permeability were examined. Visfatin was tested at 2 μg/mL which was demonstrated to generate maximal action to increase ASMase activity, activate NADPH oxidase, and induce glomerular injury. After a 6-hour treatment, visfatin induced a significant increase in the GEC permeability compared to untreated cells. This visfatin-induced increase in the GEC permeability was markedly attenuated by pretreatment with LR disruptor filipin, $gp91^{phox}$ siRNA, ASMase inhibitor amitriptyline, ASMase siRNA or adiponectin (Fig. 8). In addition, we performed experiments to detect visfatin-induced LR clustering in confluent GECs. It was found that visfatin also induced the LR clustering in confluent GECs (data was not shown).

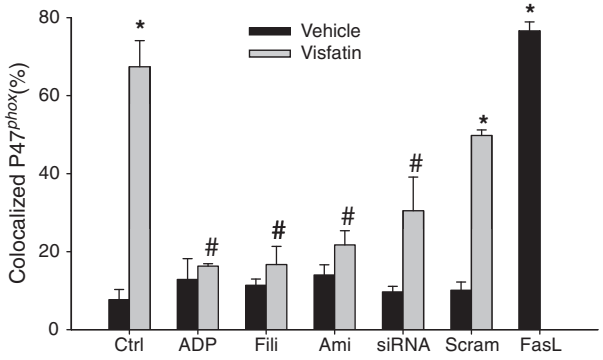

Fig. 6. Effects of adipokines on translocation of $p47^{phox}$ in GECs. Summarized data showing the effects of LR disruptor filipin, ASMase inhibitor amitriptyline and ASMase siRNA on the formation of LR-$p47^{phox}$ clusters. Panel bars display means ± SEM of five experiments with analysis of more than 1000 GECs. Ctrl: control, Ami: amitriptyline, Fili: filipin, siRNA: ASMase siRNA, Scram: scramble, and ADP: adiponectin. *P<0.05 vs. control; #P<0.05 vs. visfatin.

3.6. Involvement of cytoskeleton network in visfatin-induced GEC permeability

Using rhodamine-phalloidin as a dye for F-actin, it was found that visfatin treatment induced dramatic reorganization and disruption of the F-actin cytoskeleton in GECs compared to the control cells. In addition, to assess changes in the microtubule network in visfatin-challenged GECs, we performed immunofluorescent microscopy utilizing anti-β-tubulin antibody. It was found that there were morphological changes in microtubule network appearance upon visfatin stimulation. Upon visfatin treatment, tubulins in microtubule network were significantly reduced and remaining microtubules appear disoriented and collapsed towards the centrosome area (Fig. 9). Moreover, LR disruptor, filipin and ASMase inhibitor, attenuated the visfatin-induced microtubular network destabilization and damage.

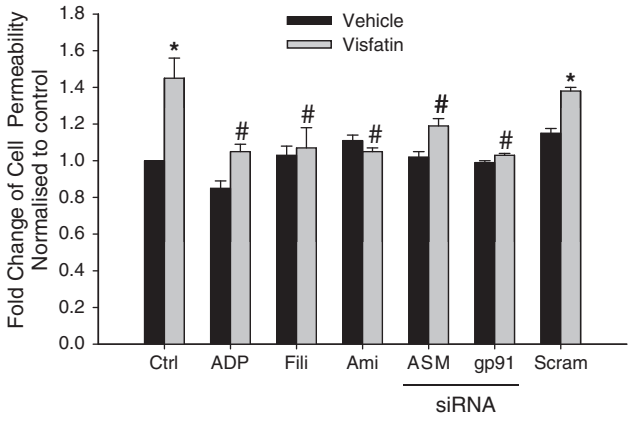

Fig. 8. Effects of adipokines on the GEC monolayer permeability. Summarized data showing the effects of adipokine-induced enhancement of GEC monolayer permeability. Ctrl: control, Ami: amitriptyline, Fili: filipin, Scram: scramble, and ADP: adiponectin. Values are means ± SEM (n = 5). *P<0.05 vs. control; #P<0.05 vs. visfatin.

4. Discussion

The main findings from our present study were that visfatin induced LR clustering in GECs as shown by the formation of larger membrane LR patches as detected by confocal microscopy. Visfatin stimulation caused an aggregation of ceramide and NADPH oxidase subunits, $gp91^{phox}$ and $p47^{phox}$ in these LR clusters, which was abolished by prior treatment with LR disruptor filipin, ASMase inhibitor amitriptyline or ASMase siRNA. Such LR clustering and NADPH oxidase subunit aggregation or recruitment form a LR redox signaling platform producing $O_2^{\bullet -}$ leading to local oxidative stress. In addition, visfatin treatment functionally increased the GEC permeability and disrupted the microtubule network. These results reveal a novel mechanism mediating visfatin-induced increase in the glomerular permeability.

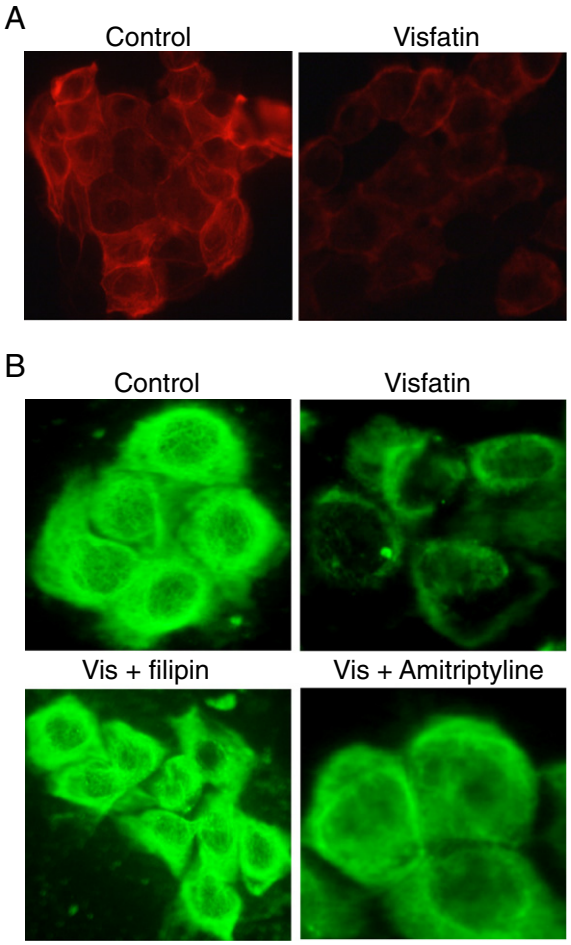

Fig. 9. Effects of adipokines on cytoskeleton network structure in GECs. Representative images of F-actin (A) and microtubule structure (B) showing the effects of visfatin, LR disruptor filipin, and ASMase inhibitor amitriptyline on cytoskeleton structure (n = 5).

Visfatin was also named as extracellular nicotinamide phosphoribosyltransferase (eNampt). Some studies have reported that visfatin (eNampt) was involved in NAD biosynthetic pathways [24]. It was reported that visfatin converted nicotinamide to nicotinamide mononucleotide (NMN), which was transported into cells through an unidentified transporter and subsequently converted to NAD by Nmnat. Recently studies from our group tested the NMN enzyme activity in other cell lines (endothelial cells) with or without treatment of visfatin using HPLC assay. We did not observe any NMN production in those cells (data was not shown). Therefore, Our results are in agreement with the observations made by Li et al., [44] that visfatin plays a role as a cytokine, but not work as a NAD biosynthetic enzyme.

Recent studies from our laboratories have demonstrated that LR clustering importantly participates in the development of endothelial dysfunction in coronary arteries, which is associated with the formation of LR redox signaling platforms [33]. The present study demonstrated that under control conditions LRs were also diffusely distributed throughout the membrane of GECs and that stimulation of these cells with visfatin resulted in a dose dependent and time dependent formation of CTX-positive fluorescent patches, which represented LR clusters or macrodomains. In the present study the LR clustering was maximal after 6 h of visfatin treatment and at a dose of 2 μg/mL visfatin. This suggests that LR clustering occurs in GECs in response to adipokines such as visfatin. However, adiponectin has no effects on the LR clustering in GECs. To our knowledge, this is the first experimental evidence that visfatin could induce LR clustering in GECs, which may have significant relevance to glomerular function.

In our previous studies, we have demonstrated that LR clustering associated with ceramide occurs in coronary endothelial cells to form the redox signaling platform on the cell membrane, which mediates NADPH oxidase activation, resulting in increased $O_2^{\bullet -}$ production and endothelial dysfunction [38]. This ceramide signaling mechanism has been reported to mediate the actions of various agonists or stimuli such as cytokines, chemotherapeutic drugs, radiation, TNF-α, interleukin 2 (IL-2) and endostatin in a variety of mammalian tissues or cells [45,46]. We hypothesized that such ceramide LR signaling pathway may also contribute to the action of visfatin on the NADPH oxidase activity in GECs and thereby mediate its role in glomerular injury. To test this hypothesis, the present study used different approaches such as confocal microscopy and liquid chromatography/mass spectrometry analysis and demonstrated that visfatin indeed significantly enhanced the ceramide production in GECs, abundant in visfatin-induced LR clusters. It is possible that this increased ceramide in GECs triggers LR clustering due to its fusagen action and forms signaling platforms when these cells are exposed to visfatin, which initiates an early event of GEC injury. As reported earlier, ceramide was importantly involved in renal glomerular and tubular pathology [47–49]. It can trigger apoptosis through a variety of intracellular targets such as ceramide-activated protein kinase (CAPK), MAP kinases, caspases, and transcription factors like NFkB. Activation of MAP kinases and caspases occurs during ischemia/reperfusion injury to kidneys [50,51]. The present study further clarified that the formation of LR redox signaling platforms or clusters in GECs is one of the important mechanisms mediating the action of ceramide in glomerular or renal injury. However, confocal fluorescent microscopy detects local enrichment of ceramide as a consequence of phase separation and/or ceramide production and does not measure absolute changes in lipid concentration.

To further explore the mechanism by which visfatin increases ceramide production in GECs, we examined the possible role of ASMase in the formation of LR redox signaling platforms and subsequent endothelial function. It was demonstrated that visfatin significantly increased the ASMase activity in a time dependent manner and the maximal ASMase activity was observed in GECs after 6 h of visfatin treatment. This visfatin-induced increase in the ASMase activity was abolished by ASMase siRNA or ASMase inhibitor, amitriptyline. This result strongly supports the view that visfatin stimulates endogenous ceramide production via activation of ASMase in GECs. Moreover, we found that visfatin-induced LR clustering was abolished in the cell membrane of ASMase gene silenced GECs or ASMase inhibitor (amitriptyline) pretreated GECs. We believe that it is ASMase product, ceramide that contributes to the formation of LR platforms in these GECs. This is consistent with earlier studies showing that ceramide was capable of triggering the fusion of LRs into larger platforms in the membrane of different type of cells [52,53].

Next we tested a hypothesis that visfatin induces or enhances NADPH oxidase activation through the formation of LR signaling platforms. By using confocal colocalization analysis of LR marker, Alexa488-labeled CTXB and Texas Red conjugated gp91^{phox} and p47^{phox}, which are two typical NADPH oxidase subunits, we demonstrated that visfatin stimulated LR clustering and enhanced enrichment of NADPH oxidase subunits in LR clusters. However, adiponectin had no such effect. These results suggest that NADPH oxidase subunits such as gp91^{phox} were aggregated in response to visfatin stimulation. To further confirm this hypothesis, we determined whether LRs are coupled to the NADPH oxidase subunits using floated detergent-resistant membrane fractions. The NADPH oxidase subunit gp91^{phox} was detected in non-LR fractions from GECs under control condition. However, stimulation of GECs with visfatin treatment significantly increased the gp91^{phox} protein in LR fractions compared to control GECs. This aggregation of NADPH oxidase subunits may play an essential role in the response of this enzyme to agonists in GECs. Although there are many studies demonstrating an assembling of NADPH oxidase subunits to form an enzyme complex and to produce $O_2\bullet^-$ [54], our findings further define a mechanism mediating such assembling of NADPH oxidase through LR clustering.

We also found that a cytosolic subunit, p47^{phox} was enriched in membrane LR fractions upon visfatin stimulation. This p47^{phox} enrichment in LR fractions represents its translocation into the cell membrane because this NADPH oxidase subunit is normally present in the cytosol. In this regard, p47^{phox} has been reported to be translocated and to then interact with membrane-bound NADPH oxidase subunits in response to agonists such as Ang II, tumor necrosis factor (TNF)-α, growth factors, and thrombin [55–57]. It is now known that this translocation of p47^{phox} is governed by serine phosphorylation and that p47^{phox} protein contains a number of phosphorylation sites for PKC, PKA, and MAPK [57]. The findings of the present study further demonstrate that this p47^{phox} translocation occurs in LR microdomains, in particular, in the LR platforms during agonist stimulations. Such LR clustering provides a driving force promoting this p47^{phox} translocation in response to agonist stimulations such as visfatin used in the present study. To provide direct evidence that aggregation or assembling of NADPH oxidase components via LR clustering is involved in activation of this enzyme, we determined NADPH oxidase-derived $O_2\bullet^-$ production in GECs using ESR technique. It was shown that visfatin indeed enhanced NADPH oxidase-dependent $O_2\bullet^-$ generation in these GECs, which was blocked by LR disruptor filipin, gp91^{phox} siRNA, ASMase inhibitor amitriptyline and ASMase siRNA. It is obvious that aggregated NADPH oxidase subunits in LR platforms are functioning as an active enzyme complex and leading to local oxidative stress. This observation is consistent with our earlier findings in coronary artery endothelial cells challenged with FasL [33,35,51] and raises the possibility that LR clustering may be an important driving force for the assembling and activation of NADPH oxidase both in endothelial and non-endothelial cells. However, it is indecisive whether these visfatin-induced changes of lipids and protein fluorescence patterns necessarily reflect the organization of these biomolecules in living systems.

To further explore the functional significance of LR redox signaling platforms in GECs, we determined the role of LR redox signaling platforms in mediating visfatin-induced enhancement of GEC monolayer permeability. It is well known that the endothelium regulating the passage of macromolecules and circulating cells from blood to tissues is a major target of oxidative stress and therefore endothelial dysfunction plays a critical role in the pathophysiology of many vascular and renal diseases [58,59]. In regard to the regulation of the vascular permeability, there is substantial evidence that oxidative stress increases the vascular endothelial permeability [60,61] and that increased endothelial and ultimate glomerular permeability importantly contributes to the development of glomerular injury and sclerosis. However, so far there is no direct evidence concerning the effect of visfatin on GEC or glomerular permeability. The present study has shown that visfatin increased the permeability of GEC monolayer in a LR clustering-dependent manner. This visfatin-induced increase in the GEC permeability was markedly attenuated by pretreatment with LR disruptor filipin, gp91^{phox} siRNA, ASMase inhibitor amitriptyline, ASMase siRNA or adiponectin. This LR clustering and consequent formation of redox signaling platforms may induce local oxidative stress and lead to increased permeability of GEC monolayer. These results for the first time link LR-mediated transmembrane signaling to the glomerular permeability through a redox regulatory mechanism and suggest that NADPH oxidase associated with LRs clustering plays an important role in mediating the effects of visfatin on the GEC permeability. Furthermore, the present study demonstrated that microtubules in GECs are organized into a lattice network with extensions from the center to the cell periphery under normal condition. The treatment of GECs with visfatin led to collapse and shortening of microtubules with reduction of assembled microtubule networks. These visfatin-induced alterations of microtubules could be blocked by inhibition of LR redox signaling platform formation and by scavenging $O_2\bullet^-$, suggesting the involvement of LR redox signaling platforms in the derangement of GEC microtubule network. In this regard, reorganization of the endothelial cytoskeleton has been reported as a molecular mechanism by which endothelial cells change their shape and intercellular gap to determine the endothelial permeability [62]. Among endothelial cytoskeleton components (microfilaments of actin, microtubules and intermediate filaments), the critical role of microtubule cytoskeleton and its cross-talk with actin network have been emphasized in many studies [61,63]. In addition, using rhodamine-phalloidin as a dye for F-actin, it was found that visfatin treatment indeed induced dramatic reorganization and disruption of the F-actin cytoskeleton in GECs compared to the control cells. These results confirm such network occurs in GECs and visfatin influences such network due to its action on LR clustering and NADPH oxidase activity.

In conclusion, the present study demonstrates a novel mechanism of visfatin-induced glomerular endothelial cell dysfunction. This mechanism is associated with assembling and activation of NADPH oxidase in ceramide-enriched domains in GECs, and the formation of this LR redox signaling platform which may mediate the pathological actions of visfatin on the glomerular endothelium by the derangement of microtubule network in GECs.

Acknowledgements

This study was supported by grants DK54927, HL075316, and HL57244 from the National Institutes of Health.

Appendix A. Supplementary data

Supplementary data to this article can be found online at doi:10.1016/j.bbalip.2010.09.001.

References

[1] R. Weiss, J. Dziura, T.S. Burgert, W.V. Tamborlane, S.E. Taksali, C.W. Yeckel, K. Allen, M. Lopes, M. Savoye, J. Morrison, R.S. Sherwin, S. Caprio, Obesity and the metabolic syndrome in children and adolescents, N. Engl. J. Med. 350 (2004) 2362–2374.

[2] S.Z. Yanovski, J.A. Yanovski, Obesity, N. Engl. J. Med. 346 (2002) 591–602.

[3] A.H. Berg, T.P. Combs, X. Du, M. Brownlee, P.E. Scherer, The adipocyte-secreted protein Acrp30 enhances hepatic insulin action, Nat. Med. 7 (2001) 947–953.

[4] T. Yamauchi, J. Kamon, H. Waki, Y. Terauchi, N. Kubota, K. Hara, Y. Mori, T. Ide, K. Murakami, N. Tsuboyama-Kasaoka, O. Ezaki, Y. Akanuma, O. Gavrilova, C. Vinson, M.L. Reitman, H. Kagechika, K. Shudo, M. Yoda, Y. Nakano, K. Tobe, R. Nagai, S. Kimura, M. Tomita, P. Froguel, T. Kadowaki, The fat-derived hormone adiponectin reverses insulin resistance associated with both lipoatrophy and obesity, Nat. Med. 7 (2001) 941–946.

[5] N. Ouchi, S. Kihara, Y. Arita, Y. Okamoto, K. Maeda, H. Kuriyama, K. Hotta, M. Nishida, M. Takahashi, M. Muraguchi, Y. Ohmoto, T. Nakamura, S. Yamashita, T. Funahashi, Y. Matsuzawa, Adiponectin, an adipocyte-derived plasma protein, inhibits endothelial NF-kappaB signaling through a cAMP-dependent pathway, Circulation 102 (2000) 1296–1301.

[6] P. Stenvinkel, A. Marchlewska, R. Pecoits-Filho, O. Heimburger, Z. Zhang, C. Hoff, C. Holmes, J. Axelsson, S. Arvidsson, M. Schalling, P. Barany, B. Lindholm, L. Nordfors, Adiponectin in renal disease: relationship to phenotype and genetic variation in the gene encoding adiponectin, Kidney Int. 65 (2004) 274–281.

[7] Y. Iwashima, T. Horio, M. Kumada, Y. Suzuki, S. Kihara, H. Rakugi, Y. Kawano, T. Funahashi, T. Ogihara, Adiponectin and renal function, and implication as a risk of cardiovascular disease, Am. J. Cardiol. 98 (2006) 1603–1608.

[8] L. Qi, A. Doria, J.E. Manson, J.B. Meigs, D. Hunter, C.S. Mantzoros, F.B. Hu, Adiponectin genetic variability, plasma adiponectin, and cardiovascular risk in patients with type 2 diabetes, Diabetes 55 (2006) 1512–1516.

[9] J.N. Fain, B.M. Tagele, P. Cheema, A.K. Madan, D.S. Tichansky, Release of 12 adipokines by adipose tissue, nonfat cells, and fat cells from obese women, Obesity 18 (2010) 890–896 (Silver.Spring).

[10] C. Zoccali, F. Mallamaci, G. Tripepi, F.A. Benedetto, S. Cutrupi, S. Parlongo, L.S. Malatino, G. Bonanno, G. Seminara, F. Rapisarda, P. Fatuzzo, M. Buemi, G. Nicocia, S. Tanaka, N. Ouchi, S. Kihara, T. Funahashi, Y. Matsuzawa, Adiponectin, metabolic risk factors, and cardiovascular events among patients with end-stage renal disease, J. Am. Soc. Nephrol. 13 (2002) 134–141.

[11] J.K. Sethi, A. Vidal-Puig, Visfatin: the missing link between intra-abdominal obesity and diabetes? Trends Mol. Med. 11 (2005) 344–347.

[12] B. Samal, Y. Sun, G. Stearns, C. Xie, S. Suggs, I. McNiece, Cloning and characterization of the cDNA encoding a novel human pre-B-cell colony-enhancing factor, Mol. Cell. Biol. 14 (1994) 1431–1437.

[13] C. Pagano, C. Pilon, M. Olivieri, P. Mason, R. Fabris, R. Serra, G. Milan, M. Rossato, G. Federspil, R. Vettor, Reduced plasma visfatin/pre-B cell colony-enhancing factor in obesity is not related to insulin resistance in humans, J. Clin. Endocrinol. Metab. 91 (2006) 3165–3170.

[14] J.R. Revollo, A.A. Grimm, S. Imai, The regulation of nicotinamide adenine dinucleotide biosynthesis by Nampt/PBEF/visfatin in mammals, Curr. Opin. Gastroenterol. 23 (2007) 164–170.

[15] D.A. de Luis, M.G. Sagrado, R. Aller, R. Conde, O. Izaola, Circulating visfatin in obese non-diabetic patients in relation to cardiovascular risk factors, insulin resistance, and adipocytokines: a contradictory piece of the puzzle, Nutrition (2009) (Epub ahead of print).

[16] A. Fukuhara, M. Matsuda, M. Nishizawa, K. Segawa, M. Tanaka, K. Kishimoto, Y. Matsuki, M. Murakami, T. Ichisaka, H. Murakami, E. Watanabe, T. Takagi, M. Akiyoshi, T. Ohtsubo, S. Kihara, S. Yamashita, M. Makishima, T. Funahashi, S. Yamanaka, R. Hiramatsu, Y. Matsuzawa, I. Shimomura, Visfatin: a protein secreted by visceral fat that mimics the effects of insulin, Science 307 (2005) 426–430.

[17] M.P. Chen, F.M. Chung, D.M. Chang, J.C. Tsai, H.F. Huang, S.J. Shin, Y.J. Lee, Elevated plasma level of visfatin/pre-B cell colony-enhancing factor in patients with type 2 diabetes mellitus, J. Clin. Endocrinol. Metab. 91 (2006) 295–299.

[18] D.G. Haider, J. Pleiner, M. Francesconi, G.F. Wiesinger, M. Muller, M. Wolzt, Exercise training lowers plasma visfatin concentrations in patients with type 1 diabetes, J. Clin. Endocrinol. Metab. 91 (2006) 4702–4704.

[19] S.D. Bailey, J.C. Loredo-Osti, P. Lepage, J. Faith, J. Fontaine, K.M. Desbiens, T.J. Hudson, C. Bouchard, D. Gaudet, L. Perusse, M.C. Vohl, J.C. Engert, Common polymorphisms in the promoter of the visfatin gene (PBEF1) influence plasma insulin levels in a French–Canadian population, Diabetes 55 (2006) 2896–2902.

[20] J. Axelsson, A. Witasp, J.J. Carrero, A.R. Qureshi, M.E. Suliman, O. Heimburger, P. Barany, B. Lindholm, A. Alvestrand, M. Schalling, L. Nordfors, P. Stenvinkel, Circulating levels of visfatin/pre-B-cell colony-enhancing factor 1 in relation to genotype, GFR, body composition, and survival in patients with CKD, Am. J. Kidney Dis. 49 (2007) 237–244.

[21] K.H. Cheng, C.S. Chu, K.T. Lee, T.H. Lin, C.C. Hsieh, C.C. Chiu, W.C. Voon, S.H. Sheu, W.T. Lai, Adipocytokines and proinflammatory mediators from abdominal and epicardial adipose tissue in patients with coronary artery disease, Int. J. Obes. (Lond.) 32 (2008) 268–274.

[22] S.G. Spiroglou, C.G. Kostopoulos, J.N. Varakis, H.H. Papadaki, Adipokines in periaortic and epicardial adipose tissue: differential expression and relation to atherosclerosis, J. Atheroscler. Thromb. 17 (2010) 115–130.

[23] K. Takebayashi, M. Suetsugu, S. Wakabayashi, Y. Aso, T. Inukai, Association between plasma visfatin and vascular endothelial function in patients with type 2 diabetes mellitus, Metabolism 56 (2007) 451–458.

[24] E. van der Veer, Z. Nong, C. O'Neil, B. Urquhart, D. Freeman, J.G. Pickering, Pre-B-cell colony-enhancing factor regulates NAD+-dependent protein deacetylase activity and promotes vascular smooth muscle cell maturation, Circ. Res. 97 (2005) 25–34.

[25] M.I. Yilmaz, M. Saglam, J.J. Carrero, A.R. Qureshi, K. Caglar, T. Eyileten, A. Sonmez, E. Cakir, M. Yenicesu, B. Lindholm, P. Stenvinkel, J. Axelsson, Serum visfatin concentration and endothelial dysfunction in chronic kidney disease, Nephrol. Dial. Transplant. 23 (2008) 959–965.

[26] C. Zoccali, Endothelial dysfunction in CKD: a new player in town? Nephrol. Dial. Transplant. 23 (2008) 783–785.

[27] G. Sommer, A. Garten, S. Petzold, A.G. Beck-Sickinger, M. Bluher, M. Stumvoll, M. Fasshauer, Visfatin/PBEF/Nampt: structure, regulation and potential function of a novel adipokine, Clin. Sci. (Lond.) 115 (2008) 13–23.

[28] J. Berndt, N. Kloting, S. Kralisch, P. Kovacs, M. Fasshauer, M.R. Schon, M. Stumvoll, M. Bluher, Plasma visfatin concentrations and fat depot-specific mRNA expression in humans, Diabetes 54 (2005) 2911–2916.

[29] J. Axelsson, J. Svensson, S. Andersson-Engels, Spatially varying regularization based on spectrally resolved fluorescence emission in fluorescence molecular tomography, Opt. Express 15 (2007) 13574–13584.

[30] J.T. Norman, L.G. Fine, Intrarenal oxygenation in chronic renal failure, Clin. Exp. Pharmacol. Physiol. 33 (2006) 989–996.

[31] H.K. Song, M.H. Lee, B.K. Kim, Y.G. Park, G.J. Ko, Y.S. Kang, J.Y. Han, S.Y. Han, K.H. Han, H.K. Kim, D.R. Cha, Visfatin: a new player in mesangial cell physiology and diabetic nephropathy, Am. J. Physiol. Renal Physiol. 295 (2008) F1485–F1494.

[32] J.R. Van Beijnum, P.T. Moerkerk, A.J. Gerbers, A.P. De Bruine, J.W. Arends, H.R. Hoogenboom, S.E. Hufton, Target validation for genomics using peptide-specific phage antibodies: a study of five gene products overexpressed in colorectal cancer, Int. J. Cancer 101 (2002) 118–127.

[33] A.Y. Zhang, F. Yi, S. Jin, M. Xia, Q.Z. Chen, E. Gulbins, P.L. Li, Acid sphingomyelinase and its redox amplification in formation of lipid raft redox signaling platforms in endothelial cells, Antioxid. Redox Signal. 9 (2007) 817–828.

[34] S. Adler, B. Eng, Integrin receptors and function on cultured glomerular endothelial cells, Kidney Int. 44 (1993) 278–284.

[35] A.Y. Zhang, F. Yi, G. Zhang, E. Gulbins, P.L. Li, Lipid raft clustering and redox signaling platform formation in coronary arterial endothelial cells, Hypertension 47 (2006) 74–80.

[36] S. Jin, Y. Zhang, F. Yi, P.L. Li, Critical role of lipid raft redox signaling platforms in endostatin-induced coronary endothelial dysfunction, Arterioscler. Thromb. Vasc. Biol. 28 (2008) 485–490.

[37] M. Fillet, J.C. Van Heugen, A.C. Servais, J. De Graeve, J. Crommen, Separation, identification and quantitation of ceramides in human cancer cells by liquid chromatography–electrospray ionization tandem mass spectrometry, J. Chromatogr. A 949 (2002) 225–233.

[38] F. Yi, A.Y. Zhang, J.L. Janscha, P.L. Li, A.P. Zou, Homocysteine activates NADH/NADPH oxidase through ceramide-stimulated Rac GTPase activity in rat mesangial cells, Kidney Int. 66 (2004) 1977–1987.

[39] C. Zhang, J.J. Hu, M. Xia, K.M. Boini, C. Brimson, P.L. Li, Redox signaling via lipid raft clustering in homocysteine-induced injury of podocytes, Biochim. Biophys. Acta 1803 (2010) 482–491.

[40] C.J. Ying, J.W. Xu, K. Ikeda, K. Takahashi, Y. Nara, Y. Yamori, Tea polyphenols regulate nicotinamide adenine dinucleotide phosphate oxidase subunit expression and ameliorate angiotensin II-induced hyperpermeability in endothelial cells, Hypertens. Res. 26 (2003) 823–828.

[41] P.L. Hordijk, E. Anthony, F.P. Mul, R. Rientsma, L.C. Oomen, D. Roos, Vascular-endothelial-cadherin modulates endothelial monolayer permeability, J. Cell Sci. 112 (Pt 12) (1999) 1915–1923.

[42] S. Jin, F. Yi, P.L. Li, Contribution of lysosomal vesicles to the formation of lipid raft redox signaling platforms in endothelial cells, Antioxid. Redox Signal. 9 (2007) 1417–1426.

[43] C.R. Bollinger, V. Teichgraber, E. Gulbins, Ceramide-enriched membrane domains, Biochim. Biophys. Acta 1746 (2005) 284–294.

[44] Y. Li, Y. Zhang, B. Dorweiler, D. Cui, T. Wang, C.W. Woo, C.S. Brunkan, C. Wolberger, S. Imai, I. Tabas, Extracellular Nampt promotes macrophage survival via a nonenzymatic interleukin-6/STAT3 signaling mechanism, J. Biol. Chem. 283 (2008) 34833–34843.

[45] E. Gulbins, Regulation of death receptor signaling and apoptosis by ceramide, Pharmacol. Res. 47 (2003) 393–399.

[46] G.S. Dbaibo, Y.A. Hannun, Signal transduction and the regulation of apoptosis: roles of ceramide, Apoptosis 3 (1998) 317–334.

[47] G.P. Kaushal, A.B. Singh, S.V. Shah, Identification of gene family of caspases in rat kidney and altered expression in ischemia–reperfusion injury, Am. J. Physiol. 274 (1998) F587–F595.

[48] N. Ueda, G.P. Kaushal, S.V. Shah, Apoptotic mechanisms in acute renal failure, Am. J. Med. 108 (2000) 403–415.

[49] T. Yin, G. Sandhu, C.D. Wolfgang, A. Burrier, R.L. Webb, D.F. Rigel, T. Hai, J. Whelan, Tissue-specific pattern of stress kinase activation in ischemic/reperfused heart and kidney, J. Biol. Chem. 272 (1997) 19943–19950.

[50] G.P. Kaushal, N. Ueda, S.V. Shah, Role of caspases (ICE/CED 3 proteases) in DNA damage and cell death in response to a mitochondrial inhibitor, antimycin A, Kidney Int. 52 (1997) 438–445.

[51] S.A. Peralta, J.M. Mullin, K.A. Knudsen, C.W. Marano, Tissue remodeling during tumor necrosis factor-induced apoptosis in LLC-PK1 renal epithelial cells, Am. J. Physiol. 270 (1996) F869–F879.
[52] E. Gulbins, H. Grassme, Ceramide and cell death receptor clustering, Biochim. Biophys. Acta 1585 (2002) 139–145.
[53] H. Grassme, V. Jendrossek, J. Bock, A. Riehle, E. Gulbins, Ceramide-rich membrane rafts mediate CD40 clustering, J. Immunol. 168 (2002) 298–307.
[54] B. Lassegue, R.E. Clempus, Vascular NAD(P)H oxidases: specific features, expression, and regulation, Am. J. Physiol. Regul. Integr. Comp. Physiol. 285 (2003) R277–R297.
[55] C. Dewas, P.M. Dang, M.A. Gougerot-Pocidalo, J. El Benna, TNF-alpha induces phosphorylation of p47(phox) in human neutrophils: partial phosphorylation of p47phox is a common event of priming of human neutrophils by TNF-alpha and granulocyte-macrophage colony-stimulating factor, J. Immunol. 171 (2003) 4392–4398.
[56] U. Landmesser, H. Cai, S. Dikalov, L. McCann, J. Hwang, H. Jo, S.M. Holland, D.G. Harrison, Role of p47(phox) in vascular oxidative stress and hypertension caused by angiotensin II, Hypertension 40 (2002) 511–515.
[57] C. Patterson, J. Ruef, N.R. Madamanchi, P. Barry-Lane, Z. Hu, C. Horaist, C.A. Ballinger, A.R. Brasier, C. Bode, M.S. Runge, Stimulation of a vascular smooth muscle cell NAD(P)H oxidase by thrombin. Evidence that p47(phox) may participate in forming this oxidase in vitro and in vivo, J. Biol. Chem. 274 (1999) 19814–19822.
[58] M. Simionescu, Implications of early structural–functional changes in the endothelium for vascular disease, Arterioscler. Thromb. Vasc. Biol. 27 (2007) 266–274.
[59] H. Lum, K.A. Roebuck, Oxidant stress and endothelial cell dysfunction, Am. J. Physiol. Cell Physiol. 280 (2001) C719–C741.
[60] W. Seeger, T. Hansen, R. Rossig, T. Schmehl, H. Schutte, H.J. Kramer, D. Walmrath, N. Weissmann, F. Grimminger, N. Suttorp, Hydrogen peroxide-induced increase in lung endothelial and epithelial permeability—effect of adenylate cyclase stimulation and phosphodiesterase inhibition, Microvasc. Res. 50 (1995) 1–17.
[61] D. Bernhard, A. Csordas, B. Henderson, A. Rossmann, M. Kind, G. Wick, Cigarette smoke metal-catalyzed protein oxidation leads to vascular endothelial cell contraction by depolymerization of microtubules, FASEB J. 19 (2005) 1096–1107.
[62] E. Tzima, Role of small GTPases in endothelial cytoskeletal dynamics and the shear stress response, Circ. Res. 98 (2006) 176–185.
[63] A.A. Birukova, K.G. Birukov, D. Adyshev, P. Usatyuk, V. Natarajan, J.G. Garcia, A.D. Verin, Involvement of microtubules and Rho pathway in TGF-beta1-induced lung vascular barrier dysfunction, J. Cell. Physiol. 204 (2005) 934–947.